JACS
JOURNAL OF THE AMERICAN CHEMICAL SOCIETY
Article
pubs.acs.org/JACS

Formation of an Unusual Four-Membered Nitrogen Ring (Tetrazetidine) Radical Cation

David Camp,*[,†] Marc Campitelli,[†] Graeme R. Hanson,[‡] and Ian D. Jenkins[†]

[†]Eskitis Institute, Griffith University, Nathan QLD 4111, Australia

[‡]Centre for Advanced Imaging, University of Queensland, St Lucia QLD 4072, Australia

Supporting Information

ABSTRACT: Treatment of triphenylphosphine (Ph_3P) with an excess of diisopropyl azodicarboxylate at 0−25 °C resulted in the formation of a symmetrical tetraalkyl tetrazetidinetetracarboxylate radical cation, containing the elusive cyclic N_4 ring system. Electron paramagnetic resonance (EPR) spectroscopy revealed a 9-line spectrum, with hyperfine coupling constants indicative of four almost magnetically equivalent nitrogen atoms. The radical species was surprisingly long-lived, and could still be observed several hours after generation and standing at 25 °C. Expansion of the central resonance revealed further splitting into a pentet (hyperfine coupling to the four methine protons). Three mechanistically plausible structures containing the tetrazetidine substructure were proposed based on the 9-line EPR spectrum. Following DFT calculations, the predicted hyperfine coupling constants were used to simulate the EPR spectra for the three candidate structures. The combined calculations and simulations were consistent with a radical cation species, but not a radical anion or radical-carbenoid structure. The lowest energy conformation of the N_4 ring was slightly puckered, with the alkyl carboxylate groups all *trans* and the four carbonyl groups aligned in a pinwheel arrangement around the ring. Analogous results were obtained with the original Mitsunobu reagents, Ph_3P and diethyl azodicarboxylate, but not with Ph_3P and di-*tert*-butyl azodicarboxylate. A mechanism is proposed based on a radical version of the Rauhut−Currier or Morita−Baylis−Hillman reactions.

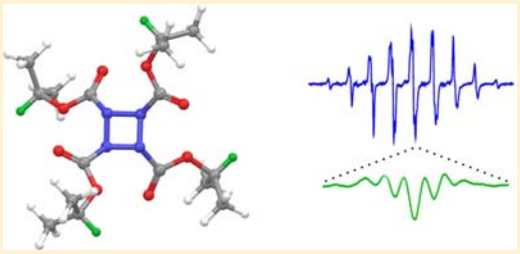

INTRODUCTION

The four-membered nitrogen ring (tetrazetidine) system **1** is one of the few simple structures in organic chemistry that has not yet been definitively synthesized. The quest to generate the homocyclic N_4 ring gained credence following the first *ab initio* molecular orbital (MO) study in 1989 of tetrazetidine (**1** , R = H).[1] This investigation accompanied the attempted thermal-

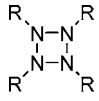

1

and photo-isomerization of diazobenzenophane in an effort to rationalize a peculiarity in the experimental results which the authors speculated could be a short-lived tetrazetidine intermediate.[1] Importantly, although the evidence for a four-membered nitrogen ring intermediate was not conclusive, the calculations nevertheless suggested that tetrazetidine was a kinetically stable molecule that might be accessed via photochemical techniques. Later structural refinements underpinned by higher level *ab initio* calculations indicated that the lowest energy conformation of tetrazetidine adopted a D_{2d} symmetry in which the four hydrogen atoms are staggered around a slightly puckered N_4 ring.[2]

The most popular synthetic approach to the tetrazetidine ring system since publication of the seminal *ab initio* investigation has been to employ rigid scaffolds incorporating proximal bisazo motifs that, in principle, should undergo [2+2] cycloaddition upon photoexcitation.[3] A major impediment to this strategy has been the facile loss of N_2. Transannular bond formation is believed to occur when at least one nitrogen atom is converted to the corresponding *N*-oxide. However, the postulated caged tetrazetidine *N*-oxide intermediates have not yet been observed directly or isolated.[4]

A 1975 paper by Nakova et al.[5] reported the formation of tetrabenzyltetrazetidine (**1** , R = Bn) from the reaction of benzylamine with sulfur at 160−170 °C, but the evidence presented for a tetrazetidine is not convincing. Interestingly, an N_4^- defect has been detected by EPR spectroscopy following UV- or γ-irradiation of single crystals of KN_3 or RbN_3 at 77 K.[6] Although data is presented that the N_4^- species is planar, it is clearly not a tetrazetidine of the type **1**.

RESULTS AND DISCUSSION

Observation of a New Radical Species. Some time ago, in a study of the formation of radicals in the Mitsunobu reaction, we observed the formation of a persistent radical by EPR spectroscopy when triphenylphosphine (Ph_3P) was mixed with an equimolar amount of diethyl azodicarboxylate (DEAD), diisopropyl azodicarboxylate (DIAD) or di-*tert*-butyl azodicarboxylate in aprotic solvents such as toluene or THF.[7] We

Received: March 28, 2012
Published: June 18, 2012

   dx.doi.org/10.1021/ja303019y | *J. Am. Chem. Soc.* 2012, 134, 16188−16196

assigned the structure of this radical species as **2**, analogous to the Morrison–Brunn–Huisgen betaine (i.e., **2** is formed by Michael-type addition of Ph_3P to the nitrogen of the azodicarboxylate[8] followed by oxidation of the betaine by an excess of the azodicarboxylate). However, a subsequent investigation by Eberson et al. using cyclic voltammetry has shown that the structure of this radical cation is more consistent with the P–O adduct **3**.[9] Eberson's evidence is compelling, and we agree with this re-assignment.

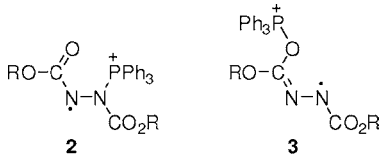

R = Et, *i*-Pr, *t*-Bu

At the time, we noticed that the EPR spectrum was dependent on the order of addition of the reagents. The cleanest signal for **3** was observed when the azodicarboxylate was added to the phosphine; when the phosphine was in excess; or when the solution was fairly dilute. However, when the phosphine was added to the azodicarboxylate, or the azodicarboxylate was in excess, or when the radical **3** was generated then treated with excess DIAD, a second radical species could be seen together with **3**. When the spectrum for **3** was subtracted from this mixed spectrum, a *new radical species* was revealed with a rather beautiful, almost symmetrical 9-line spectrum. Use of a large (5-fold) excess of DIAD and more concentrated solutions resulted in the species giving rise to the 9-line spectrum becoming the dominant radical. Thus, dropwise addition of Ph_3P (26.2 mg, 0.1 mmol) in toluene (250 μL) to neat DIAD (100 μL, 0.5 mmol) in an EPR tube under a stream of nitrogen at 25 °C afforded the EPR spectrum shown in Figure 1a after 5 min. The same spectrum could be obtained by addition of solid Ph_3P (26.2 mg) to a solution of DIAD (100 μL) in toluene (250 μL). Subsequent dilution of the sample by a factor of 4 gave the same 9-line spectrum, but with slightly improved resolution of the hyperfine structure. The radical species was surprisingly stable, the 9-line spectrum gradually decreasing in intensity over a period of 3 h. Addition of a tertiary base (triethylamine) had little effect, however, the radical decomposed immediately upon addition of a protic solvent (ethanol) or an acid (acetic or trifluoroacetic acid). The concentration of the radical species was comparable to the concentration of **3** and was estimated to be approximately 50 μM using the method employed previously.[7]

Analogous results were obtained by replacing DIAD with DEAD, which gave an almost identical 9-line spectrum (Figure 2a), however, the radical species in this case was less stable than that obtained with DIAD, and had decomposed after 45 min at 20 °C. When di-*tert*-butyl azodicarboxylate was used, only the radical species analogous to **3** was observed. There was no 9-line spectrum. When Ph_3P was replaced by tributylphosphine, an analogous 9-line spectrum was obtained with DIAD, but the EPR signal was much weaker.

EPR Studies. Double integration of each of the nine resonances within the EPR spectrum (Figure 1a) yields intensities (0.9:4.8:10.1:18.9:20.9:18.5:10.8:3.8:1.0) roughly in agreement with that expected for four magnetically equivalent nitrogen nuclei (1:4:10:16:19:16:10:4:1). Numerical differentiation of the spectra (Figures 1a, 2a) followed by Fourier filtering to remove the high frequency noise (see Experimental Section for further details) produced the second derivative spectra shown in Figures 1b and 2b, each of which exhibits enhanced resolution. An expansion of the resonances (Figures 1d, 2d–f) reveals the presence of additional proton hyperfine coupling arising from the four methine (DIAD) or eight methylene (DEAD) hydrogen nuclei, respectively. While the most intense central resonance [Figures 1d, 2e (blue)] shows an almost symmetrical splitting, this is not the case for any of the other resonances [Figures 1d, 2d,f (blue)], indicating that at least the nitrogen, and probably the hydrogen nuclei, are magnetically inequivalent, which accounts for the slight differences in the intensities mentioned above. This was confirmed through computer simulation of the EPR spectra assuming four magnetically equivalent nitrogen atoms which failed to reproduce the resonant field positions of the outermost resonances and the unsymmetrical hyperfine resonances. Computer simulation of the EPR spectra shown in Figures 1b and 2b assuming four magnetically inequivalent nitrogens and either methine (DIAD) or methylene (DEAD) protons with the spin Hamiltonian parameters given in Table 1 yields the spectra shown in Figures 1c,e and 2c,d–f (red), respectively.

Closer examination of the individual resonances, for example the three central resonances (Figures 1d, e and 2d–f), reveals

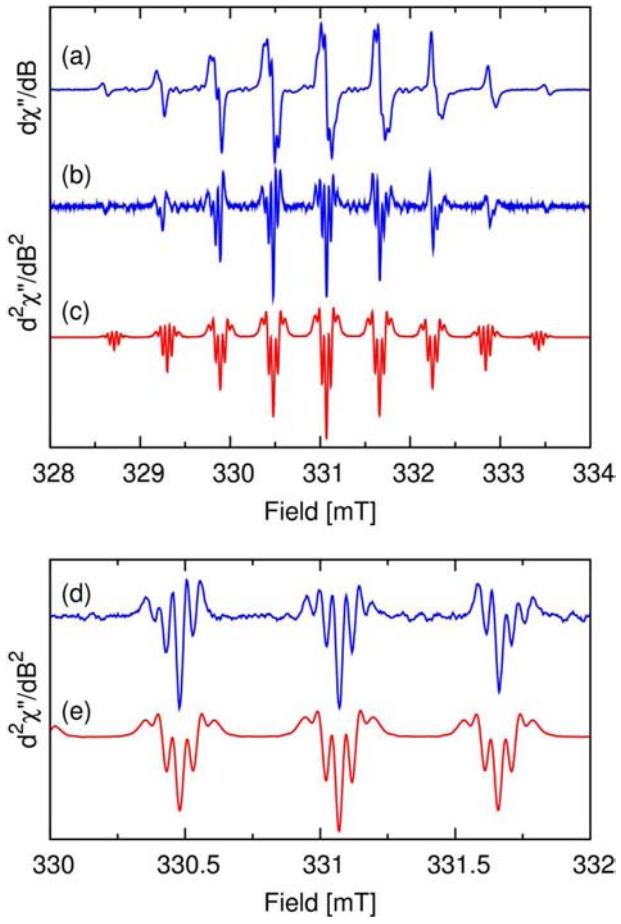

Figure 1. EPR spectrum of the radical species derived from Ph_3P and DIAD (a) Experimental first derivative spectrum, ν = 9.285814 GHz, 298 K, sample preparation details given in the text; (b) Second derivative spectrum; (c) Computer simulation using g, A_N, and A_H values given in Table 1. (d,e) Expansion of the spectra shown in (b,c), respectively revealing additional proton hyperfine coupling on the central resonances.

dx.doi.org/10.1021/ja303019y | J. Am. Chem. Soc. 2012, 134, 16188–16196

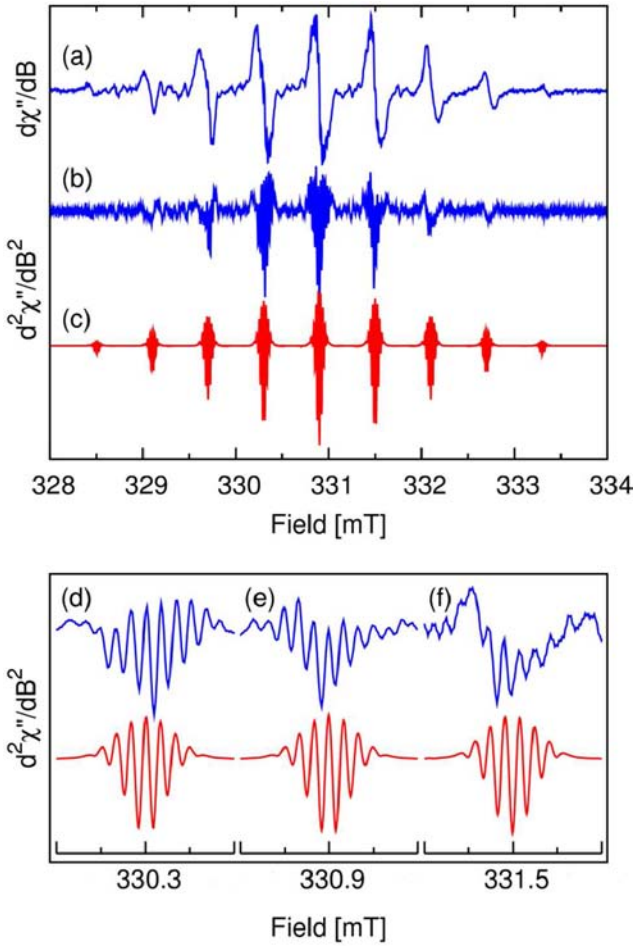

Figure 2. EPR spectrum of the radical species derived from Ph_3P and DEAD (a) Experimental first derivative spectrum, ν = 9.280583 GHz, 298 K, sample preparation details given in the text; (b) Second derivative spectrum; (c) Computer simulation of the experimental spectrum using the isotropic g, A_N, and A_H values listed in Table 1; (d–f) Expansion of the experimental (blue) and computer simulated (red) spectra shown in (b,c), revealing the additional proton hyperfine coupling. The field width of each expansion is 0.3 mT.

Table 1. Experimental Isotropic Spin Hamiltonian Parameters Determined from the Observed EPR Spectra

parameter	R = *i*-Pr	R = Et
g	2.00396	2.00388
A (^{14}N)[a]	17.361[b]	15.347
A (^{14}N)	17.298	15.347
A (^{14}N)	16.966	16.018
A (^{14}N)	16.908	16.018
A (^{1}H)[a]	1.310[c]	0.673[d]
A (^{1}H)	1.310	0.673
A (^{1}H)	1.310	0.673
A (^{1}H)	1.310	0.673

[a]Units: MHz. [b]Assignment of experimental hyperfine couplings to specific atoms is not possible. [c]Methine hydrogen, see Figure S1, Supporting Information. [d]Proton hyperfine couplings arise from two methylene protons, assumed to be magnetically equivalent as spectral resolution is inadequate to determine the individual couplings.

that the simulated spectra are in excellent agreement (least-squares error parameters: Figure 1c, 1.622×10^{-4}; Figure 2c, 1.558×10^{-5}) with the experimental spectra given the presence of small amounts of the betaine radical and the inability within the XSophe-Sophe-XeprView computer simulation software suite[10] to exactly reproduce the slow motional regime line shapes. While optimization (quadratic variation of the Hooke and Jeeves optimization algorithm[10]) of the spin Hamiltonian parameters for the radical species derived from Ph_3P and DIAD was relatively straightforward, this was not the case when DIAD was replaced by DEAD. The optimization approach we undertook for the radical species derived from DEAD involved Fourier transform of the second derivative spectrum, Fourier filtering to remove the proton frequencies followed by an inverse Fourier transform and subsequent computer simulation of the nitrogen hyperfine resonances. The proton hyperfine couplings were obtained in a similar fashion through removal of the nitrogen frequencies in the pseudo time domain spectrum. This strategy works extremely well when the nitrogen and proton hyperfine couplings are significantly different as observed for the DEAD derivative. However, utilizing the same method for the analogous radical species derived from DIAD was not as straightforward as the frequencies were not well separated in the pseudo time domain spectrum.

The inequivalence of the four nitrogen nuclei in an apparently symmetrical molecule is an interesting feature of the EPR spectra, as conformational motion and/or rapid tumbling in solution would be expected to result in four magnetically equivalent nitrogens. We believe that the magnetic inequivalence is most probably due to slow (on the EPR time-scale of nanoseconds) rotation around the N–C bonds. An NMR study of slow rotation about the N–C bonds in *N,N′*-biscarbethoxy-3,3,4,4-tetramethoxy-1,2-diazetidine provides support for this hypothesis. Four different methoxyl resonances (groups) were observed in the NMR spectrum recorded at low temperature in acetone/toluene, but only two different methoxyl resonances were found in acetone.[11] There is an interesting parallel with the results presented in this paper. In the case of **5** (R = Et) coupling to 2 × 2 inequivalent nitrogen nuclei is observed, but for **5** (R = *i*-Pr), the coupling is to four inequivalent nitrogens.

Hindered rotation around the N–C bonds of **5** is caused by a combination of steric effects; a result of the bulky (isopropyl ester) groups attached to each nitrogen, and some double bond character in the N–C bond (see Computational Chemistry section below and compare with the analogous rotation around the N–C bonds within amides, which is slow on the NMR time-scale of milliseconds). Slow rotation around the N–C bonds results in four possible rotamers (six including enantiomers). If we define a clockwise orientation (of the carbonyl groups around the ring) as +, and an anticlockwise orientation as −, the four possible rotamers would be A (+++ +); B (+++−); C (++−−) and; D (+−+−). Rotamers A and D would each have a single nitrogen environment. Rotamer C has two nitrogen environments. Rotamer B has no symmetry and so all four nitrogen atoms would be different. If all of these rotamers had comparable energies, they would occur in the ratio of 1:4:2:1 respectively (based on classic probabilities; note that rotamer B is chiral, and each enantiomer has a probability of 4/2[4]). DFT calculations suggest that the rotamers do have similar energies in acetonitrile (ε = 36.6), a solvent that might better approximate the polar environment of toluene/DIAD/Morrison–Brunn–Huisgen betaine (Table S1, Supporting Information). The energy difference between the various rotamers of **5** (R = *i*-Pr), for example, is <1 kcal mol^{-1}. The inability to exactly reproduce the EPR line shape of **5** is

dx.doi.org/10.1021/ja303019y | J. Am. Chem. Soc. 2012, 134, 16188–16196

Scheme 1. Proposed Mechanism of Formation of a Radical Cation 5 from Ph_3P and DIAD or DEAD

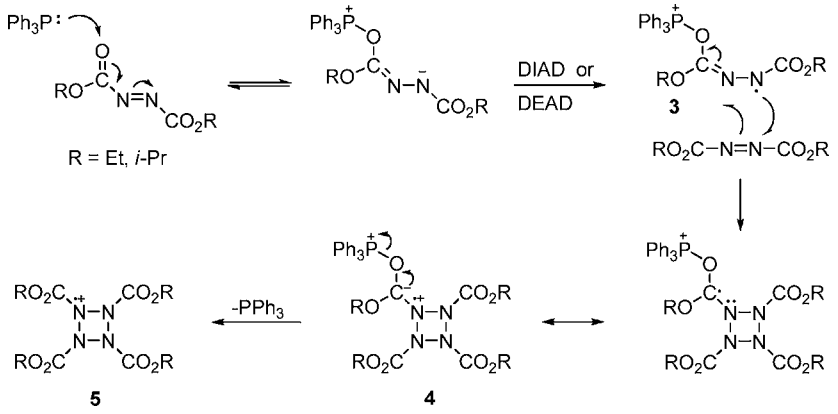

consistent with a population of rotamers (A–D) with slightly different ^{14}N,^{1}H hyperfine couplings.

Potential Species That Account for the Experimental EPR Spectrum. Three mechanistically plausible candidates were proposed for a radical giving rise to the 9-line spectrum: the symmetrical tetrazetidine radical cation **5**; the carbenoid radical cation **6**; and the radical anion **7**. A possible mechanism for the formation of the tetrazetidine radical cation **5**, based on a radical version of the Rauhut–Currier or Morita–Baylis–Hillman reactions,[12] is outlined in Scheme 1.

In Scheme 1, Michael-type addition of Ph_3P to the carbonyl oxygen of the azodicarboxylate, followed by oxidation of the resulting betaine by a second molecule of the azodicarboxylate gives the N-centered radical **3**. Radical addition of **3** to a third molecule of the azodicarboxylate followed by radical cyclization affords the intermediate **4**. Expulsion of Ph_3P with formation of the carbonyl group yields the tetrazetidine radical cation **5**. While the cleavage of a P–O bond is not commonly observed in organic chemistry, it can occur when there is a strong driving force.[13] In this case, the driving force is the formation of the carbonyl group of a carbamate [the bond dissociation energy for C=O (~175 kcal mol^{-1})[14] is greater than that for P=O (~130 kcal mol^{-1})[15]]. It should also be noted that, according to Scheme 1, the formation of **5** is catalytic in Ph_3P (as in the Rauhut–Currier or Morita–Baylis–Hillman reactions)[12] and it might be thought that two-thirds of the DEAD or DIAD would be converted into **5** (one mole of the azodicarboxylate is consumed in oxidizing the betaine to the radical cation **3**). However, the formation of **3** (the precursor of **5**) is only a very minor side reaction in the reaction of Ph_3P with an azodicarboxylate (i.e., addition of Ph_3P to the carbonyl group of DEAD or DIAD, followed by oxidation of the resulting betaine by an excess of the azodicarboxylate). The major reaction (>99.9%)[7,9] is the formation of the Morrison–Brunn–Huisgen betaine by attack of Ph_3P on the nitrogen atom of the azo moiety. This reaction is irreversible,[16] so any Ph_3P liberated during the formation of **5** would be rapidly consumed by reaction with the excess azodicarboxylate to form the (non-radical) Morrison–Brunn–Huisgen betaine.

Alternatively, the intermediate **4** could expel triphenylphosphine oxide to afford the carbenoid radical cation **6** (Scheme 2). The loss of triphenylphosphine oxide is a strong driving force for many synthetically useful reactions, but this has to be weighed against the cleavage of the C–O bond and the formation of a carbene in this case. As this is a stabilized carbene,[17] we considered that **6** should be included as a possible structure for the radical, even though it is less symmetrical than **5** and, on bond energy grounds, the formation of **5** was more likely.

Scheme 2. Possible Mechanism for Formation of a Radical Carbene 6 from Intermediate 4

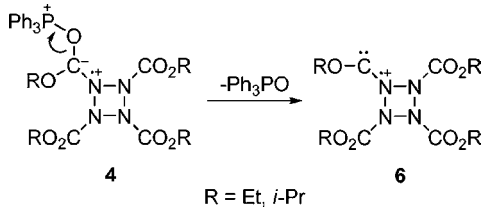

A conceivable mechanism for the formation of a radical anion **7** is outlined in Scheme 3. Single electron transfer (SET) from Ph_3P to the azodicarboxylate could afford the triphenylphosphine radical cation and the radical anion **8**, although neither species was observed by EPR under the reaction conditions. This was not unexpected in the case of the radical cation derived from Ph_3P as it has previously been reported to lack sufficient steric bulk around the phosphorus atom to afford a persistent species observable by EPR spectroscopy when generated *in situ* via anodic oxidation.[18] Radical addition of **8** to the azodicarboxylate followed by radical cyclization could, in principle, generate **7**.

Formation of the radical anion **7** seemed less likely than either the radical cation **5** or the radical carbene **6** as there was some evidence that the species giving rise to the 9-line spectrum was formed from the radical cation **3**. Thus, in some experiments when the EPR spectrum was recorded immediately after mixing the Ph_3P and the DIAD, a mixture of signals arising from **3** and the 9-line species was observed. When the spectrum was recorded again after 15–30 min, the signal for **3** had disappeared while the 9-line signal was still very strong. This observation is not due to a more rapid decomposition of **3** relative to the 9-line species, as the radical **3** has the longer half-life. Thus, when **3** is formed in the *absence* of excess DIAD, the EPR signal can still be observed some 4–5 h after generation. Similarly, when a mixture of the 9-line species containing a small amount of **3** is allowed to stand for 3 h, the signals for both species are still present, but **3** becomes the major radical present.

It should be noted that the first step in Scheme 3 (the SET to generate **8**, the most likely precursor of **7**) has been shown by Eberson to be far too endergonic to be realistic under any

dx.doi.org/10.1021/ja303019y | J. Am. Chem. Soc. 2012, 134, 16188–16196

Scheme 3. Possible Mechanism for Formation of a Radical Anion 7

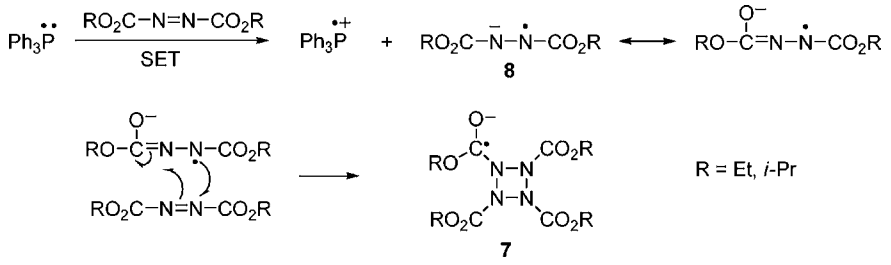

conditions.[9] It is more likely that **8** is generated during the oxidation of the betaine by DIAD or DEAD (the SET step to generate **3**, see Scheme 1). However, when **8** was generated in the presence of DIAD by other means,[7,16b] we saw no evidence of formation of the radical responsible for the 9-line spectrum.

It is also interesting to note that use of the much more sterically hindered di-*tert*-butyl azodicarboxylate (which might be expected to favor the SET process shown in Scheme 3 compared with the less sterically demanding DEAD or DIAD) only afforded the radical species **3** (R = *t*-Bu). The species giving rise to the 9-line spectrum was not observed. Presumably, the greater steric bulk of the *tert*-butyl groups prevents radical addition of **3** (R = *t*-Bu) to di-*tert*-butyl azodicarboxylate so that the tetrazetidine **5** (R = *t*-Bu) is not formed.

Computational Chemistry. Modern computational chemistry methods such as DFT have proven to be valuable tools for determining, *inter alia*, the structure of small organic molecules via prediction of their spectroscopic parameters.[19] The gas-phase optimized structures for **5**, **6**, and **7** (R = *i*-Pr) were determined at the B3LYP level of theory[20] employing the 6-31+G(d) basis set. The isopropyl analogues were chosen for the DFT calculations rather than the ethyl derivatives as the conformational flexibility of the side chains was expected (and subsequently found) to be smaller, making it easier to geometrically optimize the structure on the potential energy surface. The isotropic *g*, A_N, and A_H values for each species were then calculated from the optimized geometries using ORCA[21] in combination with the EPR-III basis set of Barone.[22] Solvation effects were included in the single point computations using the COSMO solvation model[23] and applying the dielectric constant of toluene (ε = 2.4). The predicted hyperfine coupling constants (Table 2) provide strong support for the radical cation **5** but not the alternative radical species, **6** or **7**. Subsequent simulation of the EPR spectra using the calculated values for the three candidates (Figure 3) afforded further (visual) proof. Excellent agreement was also observed between the experimental and simulated spectra for **5** (R = Et) employing the isotropic *g*, A_N, and A_H values determined empirically or via DFT calculations following the same methodology (Figure S2 and Table S2, Supporting Information).

To determine the robustness of the computational protocol, the radical cation of tetrazetidine (i.e., $\mathbf{1}^{\bullet+}$, R = H) was used as a model system to assess the performance of a range of different functionals and basis sets. The variance between the calculated structures was measured by the root-mean-square deviation (rmsd) of the atomic coordinates using the B3LYP/6-31+G(d) combination as the reference. Results ranged from 0.0032 Å [B3LYP/ccPVDZ(-f)] to 0.0248 Å [M06-HF/ccPVDZ(-f)], except for M06-2X/6-31+G(d) where a rmsd of 0.1115 Å was obtained (Table S3, Supporting Information). This could suggest that the 6-31+G(d) basis set may not be well suited to the M06-2X functional in this particular example.

Table 2. Comparison of Experimental and DFT Calculated Isotropic EPR Parameters in Toluene for 5–7 (*R* = *i*-Pr)[a]

		DFT calculated		
parameter	experimental	**5**	**6**	**7**
g	2.00396	2.0039707	2.0041402	2.0038507
A_N [N1][b]	17.361[c]	17.4775	10.3664	3.1860
A_H [H21]	1.310[c]	1.8708	−0.1551	0.0974
A_H [H33–35][d]		−0.1921	0.2670	0.0413
		−0.0266	−0.0298	0.0047
		0.2519	−0.2982	0.0304
A_H [H36–38][d]		1.0429	0.1544	0.0250
		0.5029	−0.0732	0.0337
		−0.0522	−0.3321	0.0084
A_N [N2]	17.298[c]	17.4464	22.4921	0.1868
A_H [H24]	1.310[c]	1.8911	1.4113	0.9798
A_H [H39–41][d]		−0.1906	−0.2430	−0.2616
		0.2516	0.1546	−0.0980
		−0.0263	−0.0294	0.0182
A_H [H42–44][d]		1.0494	1.0088	2.1475
		−0.0526	−0.0560	0.0062
		0.5100	0.4170	0.1226
A_N [N3]	16.966[c]	17.4451	14.7024	3.1876
A_H [H27]	1.310[c]	1.8966	1.6652	0.0975
A_H [H45–47][d]		−0.1914	0.8512	0.0251
		−0.0261	0.4428	0.0338
		0.2500	−0.0426	0.0084
A_H [H48–50][d]		1.0466	−0.1973	0.0411
		0.5127	−0.0249	0.0044
		−0.0526	0.1973	0.0305
A_N [N4]	16.908[c]	17.4510	19.6253	0.1905
A_H [H30]	1.310[c]	1.9008	1.8886	0.9853
A_H [H51–53][d]		−0.1915	0.8912	2.1540
		0.2501	−0.0401	0.0063
		−0.0262	0.5055	0.1190
A_H [H54–56][d]		1.0523	−0.1120	−0.2634
		−0.0531	0.2680	−0.0980
		0.5139	−0.0170	0.0188

[a]Units: MHz. DFT calculations employed the COSMO model with a dielectric constant appropriate for toluene (ε = 2.4). [b]Atom numbers are given in square brackets and correspond for all species to those shown in Figure S1, Supporting Information. [c]Assignment of experimental ^{14}N and ^{1}H hyperfine couplings to specific atoms is not possible. [d]The different proton hyperfine couplings for the three methyl protons will be averaged out in solution through rapid rotation of the methyl groups.

In addition, the isotropic *g*, A_N, and A_H values for the radical cations, $\mathbf{1}^{\bullet+}$ (R = H) and **5** (R = *i*-Pr and Et) were calculated in

dx.doi.org/10.1021/ja303019y | J. Am. Chem. Soc. 2012, 134, 16188–16196

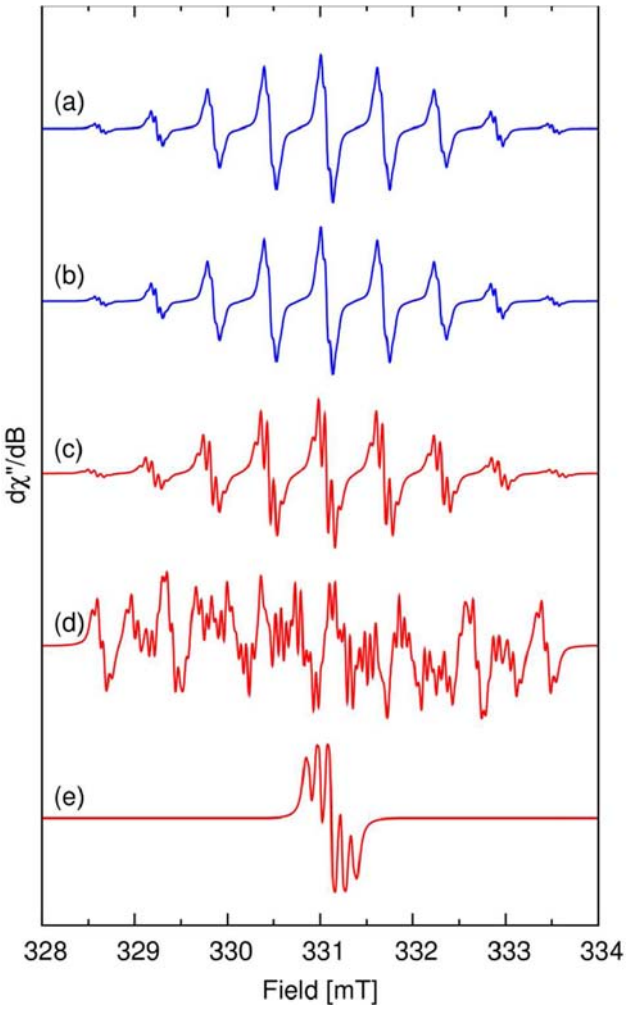

Figure 3. EPR spectra of the radical species derived from Ph_3P and DIAD (a) Experimental first derivative spectrum, ν = 9.285814 GHz, 298K; (b) Computer simulation of the experimental spectrum using the experimental isotropic g, A_N, and A_H values given in Tables 1 and 2; (c-e) Computer simulation of the EPR spectrum afforded by species **5**, **6** and **7** using the DFT calculated isotropic g, A_N, and A_H values given in Table 2. The methyl proton hyperfine couplings determined from DFT calculations were not resolved in the first and second derivative EPR spectra and were not included in the computer simulated spectra.

the gas phase, toluene and acetonitrile using the B3LYP and PBE0[24] functionals with the EPR-III basis set and COSMO solvation model where appropriate (Tables S4 and S5, respectively, Supporting Information). These results, combined with the calculated structures for $\mathbf{1}^{\bullet+}$ (R = H), indicate that the B3LYP level of theory is suitable for determining the structural and EPR parameters of **5**.

The EPR parameters for **5** (R = *i*-Pr and Et) calculated in the gas phase (ε = 0), toluene (ε = 2.4), and acetonitrile (ε = 36.6) (Table S5, Supporting Information) indicate that the long-range dielectric response of the medium produces a slight decrease in g and a small increase in A_N as the dielectric constant is increased from 0 to 36.6. Similar trends have been observed for nitroxide[25] and nitroside[26] radicals where the changes in g and A_N values are significantly larger in aqueous solutions as a consequence of hydrogen bonding.

DFT calculations employing the B3LYP/6-31+G(d) level of theory predict that the lowest energy conformation of **5** (R = *i*-Pr) is a slightly puckered four-membered ring with N−N−N bond angles of close to 90°, an N−N−N−N dihedral angle of 10.2° and pucker angle[27] of 14.5° (Table 3 and Figure 4). This

Table 3. Selected Bond Lengths and Angles of Radical Cations 5 (R = *i*-Pr and Et) and $\mathbf{1}^{\bullet+}$ (R = H) at the B3LYP/6-31+G(d) Level of Theory

parameter	**5** (R = *i*-Pr)	**5** (R = Et)	$\mathbf{1}^{\bullet+}$ (R = H)
Bond lengths[a]			
N−N	1.406	1.408	1.411
N−C	1.499	1.490	
N−H			1.029
Bond angles[b]			
N−N−N	89.5	89.6	88.5
N−N−C[c]	122.4, 119.2	122.2, 118.9	
N−N−H			115.9
Dihedral angles[b]			
N−N−N−N	10.2	10.0	18.6
N−N−N−C[c]	135.1, 137.7	134.4, 137.1	
N−N−N−H			136.7
pucker angle[b]	14.5	14.2	26.4

[a]Bond length in Å. [b]Angles in degrees. [c]The two values reflect the different orthogonal N−N bonds that can be chosen relative to the same N−C bond to measure this parameter.

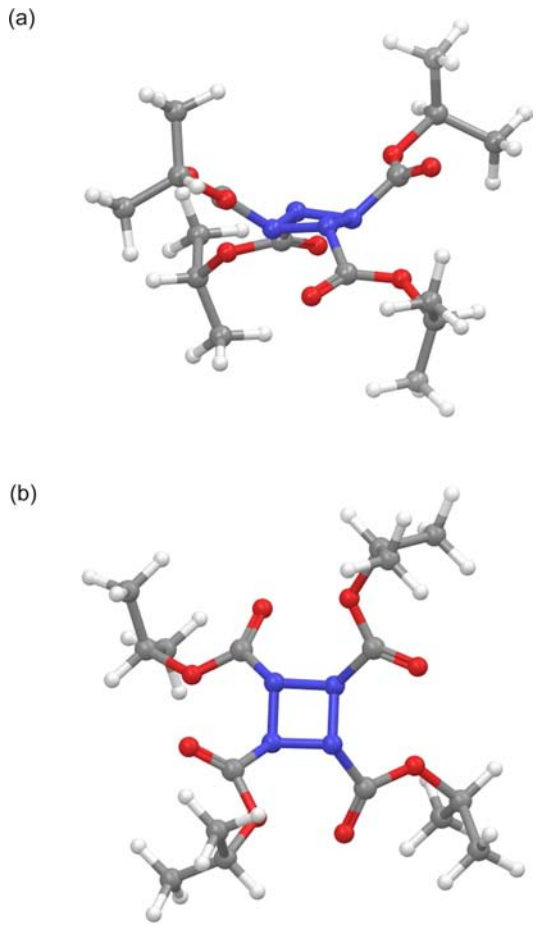

Figure 4. Lowest energy conformation (rotamer A) of the radical cation species **5** (R = *i*-Pr) oriented to show (a) the puckered N_4 ring; (b) the pinwheel arrangement of C═O moieties relative to each other.

dx.doi.org/10.1021/ja303019y | J. Am. Chem. Soc. 2012, 134, 16188−16196

is consistent with previous *ab initio* calculations for the parent tetrazetidine **1** (R = H).[2a,b] As is the case for H atoms in the lowest energy conformation for tetrazetidine,[2] the alkyl carboxylate groups in **5** are all *trans* and, interestingly, the carbonyl groups are aligned in a 'pinwheel' arrangement around the ring (i.e., rotamer A). Presumably this is a consequence of both dipolar and steric effects. As expected, the N−C bond length of ∼1.49 Å is longer than that in carbamates (∼1.37 Å),[28] reflecting the more pyramidal nature of the nitrogen atoms in **5**. Similar results were obtained for the ethyl derivative (Table 3 and Figure S3, Supporting Information). Table 3 also reports some pertinent structural parameters for the radical cation of tetrazetidine ($\mathbf{1}^{\bullet+}$, R = H). The more flattened ring in the case of **5**, as gauged by the difference in pucker angles, is most likely caused by some double bond character in the N−C bond.

SOMO. The singly occupied molecular orbital containing the unpaired electron for the radical cation **5** is shown in Figures 5

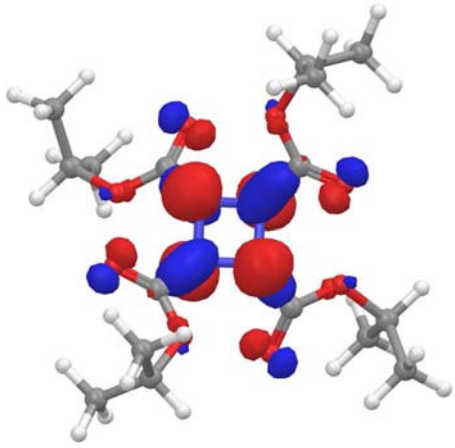

Figure 5. Depiction of SOMO for pinwheel rotamer A of the radical cation species **5** (R = *i*-Pr).

and S4 (Supporting Information) for R = *i*-Pr and Et, respectively. Interestingly, the unpaired electron is not found in a delocalized π-orbital but is restricted to one comprising the s, p_z, and p_y atomic orbitals on each of the four nitrogen nuclei. Two pairs of diametrically opposed p_z orbitals (red lobes, Figure 5) are clearly evident on each set of opposing nitrogen atoms (i.e., N1, N3 and N2, N4), and result from puckering of the tetrazetidine ring and steric crowding by the R groups.

The approximate point group symmetry of the SOMO is D_{2d} with an A_1 representation. *Ab initio* calculations performed by Ritter et al. showed that the highest occupied molecular orbital (HOMO, 16) for the neutral tetrazetidine molecule (**1** , R = H) with the same butterfly arrangement of nitrogen atoms described here for **5** (depicted as configuration 3a in their paper) also had D_{2d} symmetry with an A_1 representation that contained the lone pair of electrons.[1] Removal of an electron from the HOMO would afford a radical cation analogous to **5**. Examination of the SOMO furthermore reveals significant spin density along the N−C(C═O) bond. This leads to spin density on the methine (R = *i*-Pr) or methylene (R = Et) protons that enables proton hyperfine coupling to be observed in the EPR spectra of **5** (Figures 1 and 2). The slight inequivalence in the DFT calculated nitrogen hyperfine couplings for the pinwheel rotamer (A) of the radical cation **5** is conceivably caused by slight asymmetry in the energy-minimized structure. By way of example, the distances between the methine hydrogens in **5** (R = *i*-Pr) are all slightly different: 7.388, 7.385, 7.391, and 7.387 Å, respectively.

CONCLUSION

Treatment of Ph_3P with a concentrated solution of either DIAD or DEAD (in excess) in toluene or THF at 0−25 °C resulted in the formation of a radical species with a 9-line EPR spectrum. The combination of EPR spectroscopy and DFT calculations provides strong evidence that the radical species formed is a tetraalkyl tetrazetidinetetracarboxylate radical cation **5**, containing the elusive cyclic N_4 ring system. Slow rotation around the N−C bonds can account for the inequivalence of the four nitrogen nuclei in an apparently symmetrical molecule. The inability to exactly reproduce the EPR line shape is consistent with a population of rotamers (A−D) with slightly different ^{14}N,^{1}H hyperfine couplings. The radical was surprisingly long-lived, and could still be observed 3 h after generation and standing at room temperature. It was stable in the presence of triethylamine, but decomposed immediately upon addition of a protic solvent or acid. When DIAD was replaced by di-*tert*-butyl azodicarboxylate, the corresponding N_4 radical species was not formed. This is consistent with N_4 ring formation being subject to steric hindrance. The formation of the N_4 ring system from DIAD or DEAD is catalyzed by Ph_3P, occurs under exceptionally mild conditions, and is an unusual and unexpected new reaction in organic chemistry. A mechanism is proposed based on a radical version of the Rauhut−Currier or Morita-Baylis-Hillman reactions.[12]

EXPERIMENTAL SECTION

Materials. Triphenylphosphine, tributylphosphine, diethyl azodicarboxylate, diisopropyl azodicarboxylate, di-*tert*-butyl azodicarboxylate, triethylamine, anhydrous ethanol, acetic acid, and trifluoroacetic acid were purchased from Sigma-Aldrich and used without further purification. Toluene and THF were purchased from Merck, dried, and distilled prior to use.

Generation of Radical Cation 5. Typical procedure: neat DIAD (100 μL, 0.5 mmol) was added to an EPR tube under a stream of nitrogen at 25 °C. Ph_3P (26.2 mg, 0.1 mmol) in toluene (250 μL) was then added dropwise over 1 min under a stream of nitrogen at the same temperature. The EPR tube was sealed with a plastic cap and placed in the cavity of the spectrometer. A spectrum was recorded after approximately 5 min following addition of the first drop of Ph_3P solution.

Electron Paramagnetic Resonance Spectroscopy. Continuous wave X-band EPR spectra were recorded with Bruker Biospin ESP300e and Elexsys E500 EPR spectrometers fitted with a super high Q cavity. Magnetic field and microwave frequency calibration were achieved with a Bruker ER035 Gaussmeter and a EIP 548A microwave frequency counter (ESP300e) or a Bruker ER 036M Teslameter and a Bruker microwave frequency counter (Elexsys E500). The Elexsys E500 spectrometer tuning, signal averaging and subsequent spectral manipulations and comparisons were performed with Bruker's Xepr (version 2.6) software. Second derivative spectra were obtained by numerically differentiating the spectra and carefully Fourier filtering the resultant spectra to remove the high frequency noise without distorting the line shape. Solutions for EPR measurements were placed in standard quartz EPR tubes (Wilmad SQ707) as the dielectric loss from the solvent and compounds was minimal. Computer simulation of the experimental EPR spectra was performed with the XSophe-Sophe-XeprView computer simulation suite on a PC running Mandriva 2010.2 Linux.[10]

Computational Chemistry. Conformational searches were undertaken on the neutral progenitor for **5**-7 (R = *i*-Pr) and **5** (R = Et) using the MMFFs forcefield as implemented within MacroModel[29] on a Dell

Precision T7500 dual CPU quad core computer running under CentOS Linux (version 5.7). The two lowest energy conformations for **5**, **6**, and **7** were converted to their corresponding radicals and submitted for geometry optimization employing either the B3LYP functional[20] and 6-31+G(d) basis set [or, additionally for **5** only, the PBE0 functional[24] and ccPVTZ(-f) basis set] in the gas phase using Jaguar.[30] Default Jaguar optimization parameters were utilized with the following additional options: symmetry = off; grid density = maximum; SCF accuracy level = ultrafine; spin = unrestricted. The final geometries were characterized as an energy minimum on the potential energy surface by the absence of any imaginary vibrational frequencies at the stationary point. The EPRNMR module of ORCA[21] was used to calculate the isotropic g, A_N, and A_H EPR parameters in the gas phase or when toluene or acetonitrile was used as the solvent by running spin unrestricted B3LYP or PBE0 single point calculations in combination with the EPR-III basis set[22] at the optimized geometries employing the following input keywords: Grid5, TightSCF, COSMO(Toluene), or COSMO(Acetonitrile).[23b]

The same methodology was used to determine the lowest energy conformations of $\mathbf{1}^{\bullet+}$ (R = H) in the gas phase using Jaguar, except that an array of functionals and basis sets were employed (Table S3, Supporting Information). The structural similarity between the various combinations was determined via the rmsd of the atomic coordinates when referenced against B3LYP/6-31+G(d). Molecular properties were determined from the optimized structures derived from B3LYP/6-31+G(d) and PBE0/ccPVTZ(-f) in Jaguar. The EPRNMR module of ORCA[21] was used to calculate isotropic g, A_N, and A_H EPR parameters in the gas phase, toluene, and acetonitrile using B3LYP and PBE0 functionals in combination with the EPR-III basis set.[22]

■ ASSOCIATED CONTENT

Supporting Information

Atom numbering of radical species **5**–**7**. Experimental and simulated EPR spectra, figures of the radical cation **5** (R = Et), and its SOMO. DFT calculated spin Hamiltonian (g, A_N, and A_H) values in various solvents for $\mathbf{1}^{\bullet+}$ (R = H) and **5** (R = *i*-Pr, Et). Absolute and relative energies for rotamers of **5** (R = *i*-Pr, Et) in various solvents. Cartesian coordinates and absolute energies for $\mathbf{1}^{\bullet+}$ (R = H), **5** (R = Et), and isopropyl derivatives of **5**, **6**, and **7**. This material is available free of charge via the Internet at http://pubs.acs.org.

■ AUTHOR INFORMATION

Corresponding Author

david.camp@griffith.edu.au

Notes

The authors declare no competing financial interest.

■ ACKNOWLEDGMENTS

We thank Prof. Michael Padden-Row, Prof. Brian Roberts, Dr. Doug Brecknell, Dr. Peter Jenkins, and the late Prof. Athel Beckwith for useful discussions.

■ REFERENCES

(1) Ritter, G.; Hafelinger, G.; Luddecke, E.; Rau, H. *J. Am. Chem. Soc.* **1989**, *111*, 4627–4635.

(2) (a) Glukhovtsev, M. N.; Bach, R. D.; Laiter, S. *Int. J. Quantum Chem.* **1997**, *62*, 373–384. (b) Ball, D. W. *J. Mol. Struct. (Theochem.)* **2002**, *619*, 37–43. (c) Li, L.-C.; Shang, J.; Liu, J.-L.; Wang, X.; Wong, N.-B. *J. Mol. Struct. (Theochem.)* **2007**, *807*, 207–210.

(3) (a) Prinzbach, H.; Fischer, G.; Rihs, G.; Sedelmeir, G.; Heilbronner, E.; Yang, Y.-Z. *Tetrahedron Lett.* **1982**, *23*, 1251–1254. (b) Tauer, E.; Machinek, R. *Liebigs Ann.* **1996**, 1213–1216. (c) Cullmann, O.; Vogtle, M.; Stelzer, F.; Prinzbach, H. *Tetrahedron Lett.* **1998**, *39*, 2303–2306. (d) Fischer, G.; Fritz, H.; Rihs, G.; Hunkler, D.; Exner, K.; Knothe, L.; Prinzbach, H. *Eur. J. Org. Chem.* **2000**, 743–762. (e) Exner, K.; Fischer, G.; Bahr, N.; Beckmann, E.; Lugan, M.; Yang, F.; Rihs, G.; Keller, M.; Hunkler, D.; Knothe, L.; Prinzbach, H. *Eur. J. Org. Chem.* **2000**, 763–785.

(4) (a) Exner, K.; Prinzbach, H. *Chem. Commun.* **1998**, 749–750. (b) Exner, K.; Fischer, G.; Lugan, M.; Fritz, H.; Hunkler, D.; Keller, M.; Knothe, L.; Prinzbach, H. *Eur. J. Org. Chem.* **2000**, 787–806.

(5) (a) Nakova, E. P.; Tolkachev, O. N.; Evstigneeva, R. P. *Zh. Org. Khim.* **1975**, *11*, 2585–2589. (b) Nakova, E. P.; Tolkachev, O. N.; Evstigneeva, R. P. *J. Org. Chem. USSR* **1975**, *11*, 2660–2664. Upon dissolution in methanol, it was claimed that a minor reaction product, tetrabenzyl-1,4,2,3,5,6-dithiatetrazine, eliminated elemental sulfur to form a solid with a melting point of 232–236 °C to which the authors assigned the structure tetrabenzyltetrazetidine (**1**, R = Bn). The structure was based on the presence of only benzyl protons in the ^{1}H NMR spectrum, a m/z peak of 105 in the mass spectrum, and a microanalysis calculated for $C_{28}H_{28}N_4{\cdot}8.5H_2O$. It is unlikely that a dithiatetrazine would eliminate sulfur simply on dissolution in methanol, while a microanalysis requiring 8.5 water molecules lacks credibility.

(6) Guha, C.; Bogan, L. D.; Gilliam, O. R. *Phys. Rev. B* **1973**, *7*, 4047–4051.

(7) Camp, D.; Hanson, G. R.; Jenkins, I. D. *J. Org. Chem.* **1995**, *60*, 2977–2980.

(8) (a) Camp, D.; Healy, P. C.; Jenkins, I. D.; Skelton, B. W.; White, A. H. *J. Chem. Soc., Perkin Trans. 1* **1991**, 1323–1327. (b) Kumar, N. S.; Kumar, K. P.; Kumar, K. V. P. P.; Kommana, P.; Vittal, J. J.; Swamy, K. C. K. *J. Org. Chem.* **2004**, *69*, 1880–1889.

(9) Eberson, L.; Persson, O.; Svensson, J. O. *Acta Chem. Scand.* **1998**, *52*, 1293–1300.

(10) Hanson, G. R.; Gates, K. E.; Noble, C. J.; Griffin, M.; Mitchell, A.; Benson, S. *J. Inorg. Biochem.* **2004**, *98*, 903–916.

(11) Carlson, E. H.; Schapp, A. P.; Raban, M. *J. Org. Chem.* **1973**, *33*, 1605–1607.

(12) Mundy, B. P.; Ellerd, M. G.; Favaloro, F. G., Jr. *Name Reactions and Reagents in Organic Synthesis*, 2nd ed.; John Wiley and Sons: NJ, 2005.

(13) Petersson, M. J.; Loughlin, W. A.; Jenkins, I. D. *Chem. Commun.* **2008**, 4493–4494.

(14) Benson, S. W. *J. Chem. Educ.* **1965**, *42*, 502–515.

(15) Quin, L. D. *A Guidebook to Organophosphorus Chemistry*; Wiley Interscience: New York, 2000.

(16) (a) Crich, D.; Dyker, H.; Harris, R. J. *J. Org. Chem.* **1989**, *54*, 257–259. (b) Camp, D. Ph.D. Thesis, Griffith University, 1990.

(17) Bourissou, D.; Guerret, O.; Gabba'i, F. P.; Bertrand, G. *Chem. Rev.* **2000**, *100*, 39–91.

(18) Culcasi, M.; Berchadsky, Y.; Gronchi, G.; Tordo, P. *J. Org. Chem.* **1991**, *56*, 3537–3542.

(19) (a) Neese, F.; Munzarova, M. L. Historical Aspects of EPR Parameter Calculations. In *Calculation of NMR and EPR Parameters: Theory and Applications*; Kaupp, M., Bühl, M., Malkin, V.,, Eds.; Wiley-VCH: Weinheim, 2004, pp 21–32. (b) Neese, F. Spin Hamiltonian Parameters from First Principle Calculations: Theory and Application. In *Biological Magnetic Resonance*;; Hanson, G. R., Berliner, L. J., Eds.; Springer: New York, 2009; Vol. *28*, pp 175–232. (c) Tumanskii, B.; Pine, P.; Apeloig, Y.; Hill, N. J.; West, R. *J. Am. Chem. Soc.* **2004**, *126*, 7786–7787. (d) Tumanskii, B.; Pine, P.; Apeloig, Y.; Hill, N. J.; West, R. *J. Am. Chem. Soc.* **2005**, *127*, 8248–8249. (e) Saielli, G.; Bagno, B. *Org. Lett.* **2009**, *11*, 1409–1412. (f) Saielli, G.; Nicolaou, K. C.; Ortiz, A.; Zhang, H.; Bagno, B. *J. Am. Chem. Soc.* **2011**, *133*, 6072–6077. (g) Felippe, L. G.; Batista, J. M., Jr.; Baldoqui, D. C.; Nascimento, I. R.; Kato, M. J.; He, Y.; Nafied, L. A.; Furlan, M. *Org. Biomol. Chem.* **2012**, *10*, 4208–4214.

(20) (a) Becke, A. D. *Phys. Rev. A* **1988**, *38*, 3098–3100. (b) Becke, A. D. *J. Chem. Phys.* **1993**, *98*, 5648–5652. (c) Lee, C. T.; Yang, W. T.; Parr, R. G. *Phys. Rev. B* **1988**, *37*, 785–789.

(21) Neese, F. *ORCA—an ab initio, Density Functional and Semiempirical program package*, version 2.7; University of Bonn, 2008.

(22) Rega, N.; Cossi, M.; Barone, V. *J. Chem. Phys.* **1996**, *105*, 11060–11067.

(23) (a) Klamt, A.; Schuurmann, G. *J. Chem. Soc., Perkin Trans. 2* **1993**, 799−805. (b) Sinnecker, S.; Rajendran, A.; Klamt, A.; Diedenhofen, M.; Neese, F. *J. Phys. Chem. A* **2006**, *110*, 2235−2245.
(24) (a) Perdew, J. P.; Burke, K.; Ernzerhof, M. *Phys. Rev. Lett.* **1996**, *77*, 3865−3868. (b) Perdew, J. P.; Burke, K.; Ernzerhof, M. *Phys. Rev. Lett.* **1997**, *78*, 1396 (errata). (c) Adamo, C.; Barone, V. *J. Chem. Phys.* **1999**, *110*, 6158−6170.
(25) (a) Pavone, M.; Benzi, C.; De Angelis, F.; Barone, V. *Chem. Phys. Lett.* **2004**, *395*, 120−126. (b) Owenius, R.; Engstrom, M.; Lindgren, M.; Huber, M. *J. Phys. Chem. A* **2001**, *105*, 10967−10977.
(26) Barone, V. *Chem. Phys. Lett.* **1996**, *262*, 201−206.
(27) Kummli, D. S.; Frey, H. M.; Leutwyler, S. *J. Phys. Chem. A* **2007**, *111*, 11936−11942.
(28) (a) Kaur, D.; Sharma, P.; Bharatam, P. V. *J. Mol. Struct. (Theochem.)* **2005**, *757*, 149−153. (b) Kaur, D.; Kaur, R. P. *J. Mol. Struct. (Theochem.)* **2008**, *858*, 94−100.
(29) *MacroModel*, version 9.9; Schrodinger, LLC: New York, NY, 2011.
(30) *Jaguar*, version 7.8; Schrodinger, LLC: New York, NY, 2011.